

A class of steady solutions to two-dimensional free convection*

Sadayoshi Toh and Takeshi Matsumoto

*Division of Physics and Astronomy, Graduate School of Science, Kyoto University,
Kitashirakawa Oiwakecho Sakyo-ku, Kyoto 606-8502, Japan*

(Dated: November 16, 2018)

We obtained steady solutions to the two-dimensional Boussinesq approximation equations without mean temperature gradient. This system is referred to as free convection in this paper. Under an external flow described by the stream function $\Psi = -Ayf(x)$, two types of steady solutions are found depending on the boundary conditions. One is kept steady by the balance between the strain of Ψ and the diffusion. The solution is similar to the Burgers vortex layer solution. The other is done by the balance between vorticity induced by the buoyancy and vorticity flux caused by the external flow. Detailed argument on these two balances is presented for $f(x) = x$. Then two examples other than $f(x) = x$ are shown to have either of the two balancing mechanism. We discuss the relation between these solutions and long-lived fine scale coherent structures observed in direct numerical simulations of two-dimensional free convection turbulence.

PACS numbers: 47.27.-i, 47.27.Te, 47.32.Cc

I. INTRODUCTION

Rayleigh–Bénard convection is very rich in nature. It has been a source of inspiration in studies of universality in the route to turbulence [1]. At the same time, there have been extensive researches both experimental and theoretical on turbulent states of convection [2].

Recently, convection turbulence has attracted attention as a good example of active scalar systems. One interesting observation is scaling behavior of structure functions of temperature, active scalar. In this context, a two-dimensional Boussinesq convection model has been studied by direct numerical simulations (DNS) in a doubly periodic square domain. The results indicate that the scaling exponents of the temperature structure functions saturate as the order goes to infinity [3, 4]. It has been pointed out that coherent structures like plumes or sharp interfaces (shocks) between hot and cold regions can play an important role in this behavior. Moreover it is shown phenomenologically [5] and numerically [6] that the temperature variance (entropy [5]) cascades from larger scales to smaller scales in the turbulent two-dimensional Boussinesq system (referred to as two-dimensional free convection, 2DFC) when the turbulent state is maintained by a large scale temperature forcing. However, the relation between the entropy cascade and the dynamics of coherent structures, if any at all, is still far from understood.

In the three-dimensional Navier-Stokes (3DNS) turbulence, vortical fine coherent structures, so-called worms, are observed. These worms are well known to be approximated locally by the Burgers vortex tube. In this sense, 2DFC turbulence is quite similar to 3DNS turbulence, although the former is more feasible than the latter. We expect that the understanding of the former may help

us understand the latter and also elucidate the universal characteristics of turbulence.

The motivation of this paper is to explain some properties of the long-lived coherent structures observed in DNS in terms of a class of steady solutions of 2DFC. For this we search for steady solutions to the incompressible two-dimensional Boussinesq approximation equations without mean temperature gradient (2DFC):

$$\partial_t T + (\mathbf{u} \cdot \nabla) T = \kappa \Delta T, \quad (1)$$

$$\partial_t \mathbf{u} + (\mathbf{u} \cdot \nabla) \mathbf{u} = -\frac{\nabla p}{\rho_0} + \alpha g T \hat{\mathbf{e}} + \nu \Delta \mathbf{u}, \quad (2)$$

$$\nabla \cdot \mathbf{u} = 0. \quad (3)$$

Here κ , ρ_0 , α , g , and ν are the molecular diffusivity, the mean density of the fluid (we take ρ_0 to be unity for simplicity), the thermal expansion coefficient, the gravitational acceleration and the kinematic viscosity, respectively. The vector $\hat{\mathbf{e}}$ is the unit vector in the direction opposite to the gravity. In DNS of free convection turbulence, to keep the system statistically stationary, a large-scale forcing term is added to Eq.(1), but the details are not mentioned here.

In the turbulent temperature field, long-lived sharp interfaces between hot and cold regions, i.e. shock fronts are often formed and regarded as coherent structures. Thus coherent structures are highly elongated; The typical length is the order of the integral scale and the typical width the order of ten times of Kolmogorov dissipation length scale. We expect that steady solutions to Eqs. (1)-(3) have common properties with the coherent structures formed spontaneously in DNS.

To deal with temperature shocks more directly, we use the following vector quantity [7, 8]:

$$\boldsymbol{\chi} = (\partial_y T, -\partial_x T). \quad (4)$$

We call $\boldsymbol{\chi}$ T-vorticity. T-vorticity obeys the following evolution equation similar to the three-dimensional vorticity equation:

$$\partial_t \boldsymbol{\chi} + (\mathbf{u} \cdot \nabla) \boldsymbol{\chi} = (\boldsymbol{\chi} \cdot \nabla) \mathbf{u} + \kappa \Delta \boldsymbol{\chi}. \quad (5)$$

*submitted to *Phys.Rev.E*

Thus T-vorticity is expected to play an essential role in turbulence like vorticity in 3DNS. In contrast with T-vorticity, the governing equation for the vorticity $\omega(x, y, t)$ in 2DFC can be written

$$\partial_t \omega + (\mathbf{u} \cdot \nabla) \omega = \alpha g \{ \nabla \times (T \hat{\mathbf{e}}) \}_z + \nu \Delta \omega. \quad (6)$$

Here $\{\cdot\}_z$ denotes taking the z -component. Note that because of the buoyancy term, i.e. the first term in the r.h.s. of Eq.(6), vorticity is not a conservative quantity even for $\nu = 0$. For simplicity, we assume $\nu = \kappa$, i.e. Prandtl number $Pr = \nu/\kappa = 1$ here.

In the following sections, we look for steady solutions to Eqs. (5) and (6), where the flow is decomposed into the external part given by a stream function $\Psi = -A y f(x)$ and a response to it. In section II, we deal with the case $f(x) = x$, i.e. a stagnation flow. In Section III, extended stagnation flows, $f(x) \neq x$, are considered, where we show two examples of $f(x)$. The realizability of the extended external flow is discussed. Concluding remarks are made in Section IV.

II. BURGERS VORTEX LAYER TYPE SOLUTIONS

We assume that the system (5) and (6) is exposed to a stagnation flow

$$\Psi(x, y) = -Axy, \quad (7)$$

where A is a positive constant so that we take the directions of contraction and expansion as x -axis and y -axis, respectively. The angle between x -axis and $\hat{\mathbf{e}}$ is also a parameter and denoted by φ as shown in Fig. 1. Then the unit vector $\hat{\mathbf{e}}$ in Eq. (1) is given in this coordinate as $\hat{\mathbf{e}} = (\cos \varphi, \sin \varphi)$. We use this coordinate throughout this paper. We further assume the following forms of the temperature and velocity fields:

$$T(x, y, t) = \theta(x), \quad (8)$$

$$\begin{aligned} \mathbf{u}(x, y, t) &= (\partial_y \Psi(x, y), -\partial_x \Psi(x, y)) + (0, v(x)) \\ &= (-Ax, Ay + v(x)). \end{aligned} \quad (9)$$

In terms of θ and v , T-vorticity and vorticity are expressed as

$$\chi(x, y, t) = (0, -\partial_x \theta(x)) \equiv (0, \chi_y(x)), \quad (10)$$

$$\omega(x, y, t) = \omega(x) = \frac{dv(x)}{dx}. \quad (11)$$

Consequently, Eqs. (5) and (6) are reduced to the following ordinary differential equations:

$$\frac{d}{dx} \left(\frac{\kappa}{A} \frac{d\chi_y}{dx} + x\chi_y \right) = 0, \quad (12)$$

$$\frac{\nu}{A} \frac{d^2 \omega}{dx^2} + x \frac{d\omega}{dx} = \chi_y \frac{\alpha g \sin \varphi}{A}. \quad (13)$$

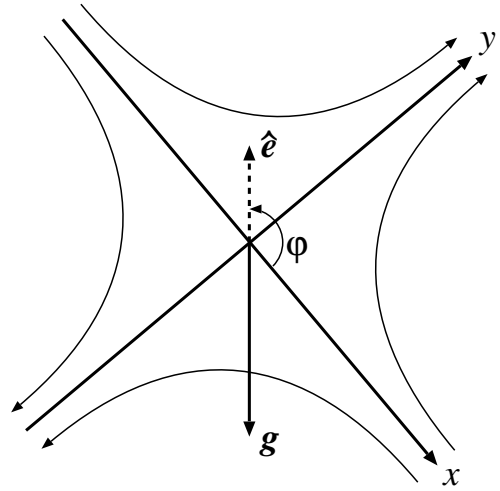


FIG. 1: The coordinate system fixed on the external stagnation flow. The direction of the gravity vector \mathbf{g} is expressed via the angle φ .

After integrating once, Eq.(12) can be written

$$\frac{\kappa}{A} \frac{d\chi_y}{dx} + x\chi_y = C. \quad (14)$$

Here C is an integration constant.

Let us consider the general boundary conditions at the origin:

$$\chi_y(x=0) = \chi_0, \quad (15)$$

$$\chi'_y(x=0) = \chi'_0, \quad (16)$$

$$\omega(x=0) = \omega_0, \quad (17)$$

$$\omega'(x=0) = \omega'_0, \quad (18)$$

where $\chi'_y(x)$ and $\omega'(x)$ denote the derivatives of T-vorticity and vorticity respectively; $\chi_0, \chi'_0, \omega_0$ and ω'_0 are constants. These conditions yield the relation $C = \kappa \chi'_0 / A$. With $\kappa = \nu$ the solutions to Eqs.(12) and (13) are obtained

$$\chi_y(x) = \chi_0 e^{-\frac{A}{2\kappa} x^2} + \chi'_0 e^{-\frac{A}{2\kappa} x^2} \int_0^x e^{\frac{A}{2\kappa} \xi^2} d\xi, \quad (19)$$

$$\begin{aligned} \omega(x) &= \omega_0 + \omega'_0 \int_0^x e^{-\frac{A}{\kappa} \xi^2} d\xi + \chi_0 \frac{\alpha g \sin \varphi}{A} (1 - e^{-\frac{A}{2\kappa} x^2}) \\ &\quad + \chi'_0 \frac{\alpha g \sin \varphi}{A} \int_0^x d\zeta e^{-\frac{A}{\kappa} \zeta^2} \int_0^\zeta d\mu \int_0^\mu d\xi e^{\frac{A}{2\kappa} \xi^2}. \end{aligned} \quad (20)$$

Here only the last two terms of Eq.(20) are the buoyancy generated vorticity. The first two are homogeneous solutions, i.e., the solutions to the vorticity equation (13) setting the r.h.s. (the buoyancy force) zero. When $\chi'_0 = 0$, the solution (19) which is the same as the Burgers vortex layer, takes finite value of temperature at $x = \pm\infty$. We call this solution finite temperature (FT) type solution. In contrast, when $\chi'_0 \neq 0$, the temperature corresponding to the solution (19) diverges as $x \rightarrow \pm\infty$. We then

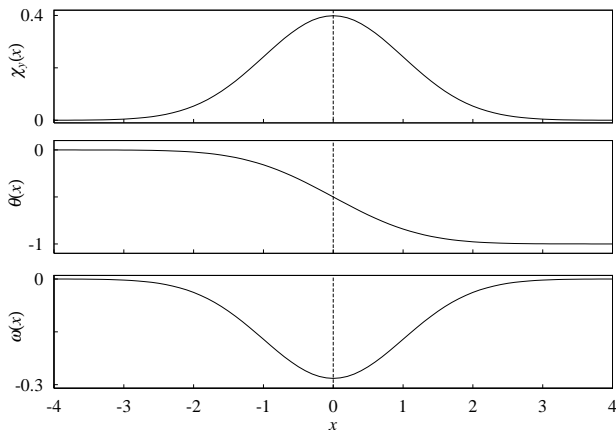


FIG. 2: Finite temperature (FT) solutions: the T-vorticity Eq.(23), the corresponding temperature $\theta(x)$ and the vorticity Eq. (24). Here we set the parameters as $\Theta_0 = 1, A = 1, \kappa = 1, \alpha g = 1$ and $\varphi = \pi/4$.

call this solution infinite temperature (IT) type solution. We treat the two cases separately in the following subsections.

A. Finite temperature type solutions

Let us consider the following boundary conditions:

$$\chi_y(x) \rightarrow 0 \quad (x \rightarrow \pm\infty), \quad (21)$$

$$\omega(x) \rightarrow 0 \quad (x \rightarrow \pm\infty). \quad (22)$$

These conditions (21) and (22) are equivalent to $\chi'_0 = 0$ and $\omega'_0 = 0$. The general solutions (19) and (20) are then reduced to Burgers vortex layer type solution:

$$\chi_y(x) = \Theta_0 \sqrt{\frac{A}{2\pi\kappa}} \exp\left(-\frac{A}{2\kappa}x^2\right), \quad (23)$$

$$\begin{aligned} \omega(x) &= -\frac{\alpha g \sin \varphi}{A} \Theta_0 \sqrt{\frac{A}{2\pi\kappa}} \exp\left(-\frac{A}{2\kappa}x^2\right) \\ &= -\frac{\alpha g \sin \varphi}{A} \chi_y(x), \end{aligned} \quad (24)$$

where $\Theta_0 = \int_{-\infty}^{\infty} \chi_y(\xi, t=0) d\xi = \theta(-\infty, 0) - \theta(\infty, 0)$. In the Burgers vortex layer, this temperature difference corresponds to the circulation of the vortex layer. In Fig. 2 we plot the solutions; T-vorticity (23), and the corresponding temperature $\theta(x)$ and vorticity (24). As mentioned before, the temperature takes finite value at $x = \pm\infty$. Since the temperature $\theta(x)$ is a monotonic function, $\chi_y(x)$ contains a single bump. We call this solution Burgers T-vortex layer solution.

Now we make several remarks on the FT solutions (23) and (24). First, we note that $\omega(x)$ is proportional to $\chi_y(x)$ and $\sin \varphi$. That is, $\chi_y(x)$ is independent of the direction of the gravity, but $\omega(x)$ is not. This is because the former is maintained by the balance between

the imposed strain and the diffusion of T-vorticity like the Burgers vortex layer solution to the 3DNS equations and the latter does by the balance between the diffusion of vorticity and the buoyancy induced by the temperature difference across the Burgers T-vortex layer. Therefore vorticity is maximized when the direction of the T-vortex layer coincides with that of the gravity.

Secondly, it is possible to estimate a characteristic time of the relaxation to the steady state (23) after the temperature difference Θ_0 is fixed. Under the stagnation flow (9), the time-dependent solution to Eq. (5) is obtained [9] as

$$\begin{aligned} \chi_y(x, t) &= \left(4\pi\kappa \frac{1 - e^{-2At}}{2A}\right)^{-1/2} \\ &\times \int_{-\infty}^{\infty} \chi_y(\xi, t=0) \exp\left[-\frac{(x - e^{-At}\xi)^2}{4\kappa \frac{1 - e^{-2At}}{2A}}\right] d\xi \\ &\rightarrow \Theta_0 \sqrt{\frac{A}{2\pi\kappa}} \exp\left(-\frac{A}{2\kappa}x^2\right) \quad \text{as } t \rightarrow \infty. \end{aligned} \quad (25)$$

The characteristic time for the relaxation is thus estimated as $1/A$.

Thirdly, the characteristic width of the bump of T-vorticity and vorticity is $\sqrt{2\kappa/A}$. This agrees with an observation about structures of a passive scalar advected by a two-dimensional synthetic random velocity field with a finite correlation time in Ref. [10]. (Of course, vorticity is not considered in that case.) Although a passive scalar with non-zero mean gradient was considered, the solution (23) may describe locally coherent structures of the passive scalar because of the following features: The width of those was found to scale well with $\sqrt{\kappa/s}$, where s was a root mean square of the rate of strain calculated from the low-path filtered velocity. They also showed a stagnation flow accompanied by a coherent structure in Fig. 7 of Ref. [10].

Finally, concerning the relevance of the FT solutions (23) and (24) to the coherent structures observed in DNS of free convection turbulence, we refer the reader to Ref. [11]. Here suffice it to say that the solutions (23) and (24) can give a good local approximation of the coherent structures in DNS, where we compared A with the (positive) eigen-value of the velocity-gradient tensor although the latter is defined only locally.

However, it is well-known that, in the limit of $\kappa \rightarrow 0$, the temperature dissipation rate per unit length along y -axis, ϵ_θ , of the Burgers (FT type) solution (23) vanishes. That is, $\epsilon_\theta = \int_{-\infty}^{\infty} \kappa \chi_y(x)^2 dx \propto \sqrt{\kappa A} \rightarrow 0$ as $\kappa \rightarrow 0$. It suggests that this Burgers layer type solution is irrelevant in this limit. In DNS, however, the situation can be different because we have to consider feedback to A (the eigen-value of the velocity-gradient tensor) from other ingredients of the flow. Indeed, the probability distribution functions of $A(x, y)$ obtained in DNS of various κ 's are observed to fall into a unique curve under a suitable normalization. In other words, $A(x, y)$ field may have some nontrivial dependency on κ . Thus it is conjectured that

the dissipation rate of the FT type solution (23), $\sqrt{\kappa A}$, would take non-zero value in the limit of vanishing diffusivity in real flows. Therefore the relevance of the Burgers vortex layer type solutions might not be ruled out. The detail of the observation on $A(x, y)$ field in DNS will be reported elsewhere.

B. Infinite temperature type solutions

In this subsection, we consider the case where the temperature slowly diverges as $x \rightarrow \pm\infty$, which we call infinite temperature type solutions. In terms of the boundary conditions at the origin, it corresponds to

$$\chi_y(x=0) = 0, \quad (26)$$

$$\chi'_y(x=0) = \chi'_0, \quad (27)$$

$$\omega(x=0) = 0, \quad (28)$$

$$\omega'(x=0) = 0, \quad (29)$$

where $\chi'_0 \neq 0$. We set $\chi_0 = 0$ to examine an IT type solution solely. The general solutions (19) and (20) then take the form:

$$\chi_y(x) = \chi'_0 e^{-\frac{A}{2\kappa}x^2} \int_0^x e^{\frac{A}{2\kappa}\xi^2} d\xi, \quad (30)$$

$$\omega(x) = \chi'_0 \frac{\alpha g \sin \varphi}{A} \int_0^x d\zeta e^{-\frac{A}{2\kappa}\zeta^2} \int_0^\zeta d\mu \int_0^\mu d\xi e^{\frac{A}{2\kappa}\xi^2} \quad (31)$$

The boundary conditions for the vorticity (28) and (29) are chosen to involve only the buoyancy effect on vorticity since we focus on the vortical structure induced by the buoyancy. It should be noted that the homogeneous solutions of Eq.(13) are neglected. We plot the IT solutions: T-vorticity Eq.(30), the corresponding temperature $\theta(x)$ and vorticity Eq.(31) in Fig. 3.

It should be noted that unlike the Burgers type solutions T-vorticity and vorticity of IT type solutions take the same sign around χ -bumps. This behavior seems to contradict physical intuition that hot fluid rises and then vorticity with the sign opposite to that of T-vorticity is induced. However, vorticity is maintained by the balance between the buoyancy and not only the diffusion of vorticity but the vorticity transfer by a stagnation flow. In fact, if vorticity takes non-zero value with the same sign of T-vorticity, say positive, at infinity, vorticity flux $Ax\omega$ through a region with the width δ centered at some point ,e.g. x_0 , always increases vorticity in the region. The substantial increase in vorticity Q_ω is given by

$$\begin{aligned} Q_\omega &= F_u - F_d \\ &= A \left(x_0 + \frac{\delta}{2} \right) \omega \left(x_0 + \frac{\delta}{2} \right) - A \left(x_0 - \frac{\delta}{2} \right) \omega \left(x_0 - \frac{\delta}{2} \right) \\ &= A\delta\omega(x_0) + A\delta x_0\omega'(x_0), \end{aligned} \quad (32)$$

where the first term in the r.h.s balances with the vorticity flux in y and the second term does with $F_\chi = \delta\chi_y(x_0)\alpha g \sin \varphi/A$ if $\omega''(x_0)$ is negligible in Eq.(13) as

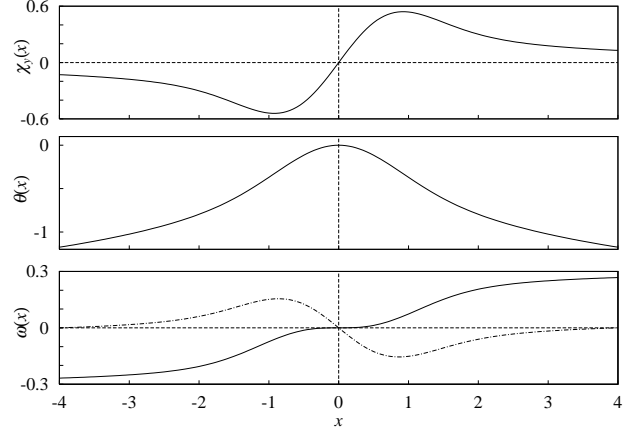


FIG. 3: Infinite temperature (IT) solutions: the T-vorticity Eq.(30), the corresponding temperature $\theta(x)$ and the vorticity Eq.(31). Here we set the parameters as $A = 1, \kappa = 1, \alpha g = 1, \varphi = \pi/4, \chi'_0 = 1, \theta(x=0) = 0, \omega'_0 = 0$ and $\kappa = 1$. The dash-dotted line in the vorticity figure is a localized vorticity solution Eq.(33) obtained by setting $\omega'_0 = -0.23$.

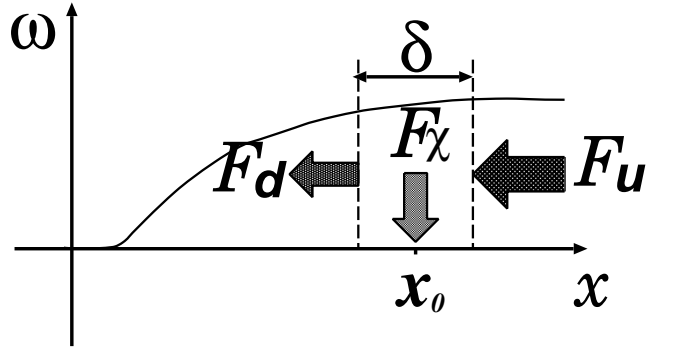


FIG. 4: Schematic view of vorticity balance in a region with the width δ centered at x_0 . $F_u = A(x_0 + \delta/2)\omega(x_0 + \delta/2)$ and $F_d = -A(x_0 - \delta/2)\omega(x_0 - \delta/2)$ are vorticity fluxes in x by a stagnation flow. $F_\chi = \delta\chi_y(x_0)\frac{\alpha g \sin \varphi}{A}$ is vorticity induced by the buoyancy.

shown in Fig. 4. That is, vorticity induced by the buoyancy cancels out the excess of the vorticity flux. On the other hand, if the sign of vorticity around infinity is opposite to that of T-vorticity, the excess of the vorticity flux cannot be canceled out by the vorticity induced by the buoyancy so that the vorticity is not kept steady.

When vorticity is localized around the origin, i.e., vanishes rapidly as x goes to infinity, the vorticity transfer is turned off and the vorticity induced by the buoyancy works as the vorticity input which balances with the diffusion of vorticity. This means that to keep the vorticity steady, $\omega(\infty)$ should be null or take the same sign as that of the T-vorticity. Even in the IT case, using the homogeneous solution to Eq.(13), vorticity can be localized around the origin. In Fig. 3 with dash-dotted line, we show this localized vorticity, which consists of the

buoyancy-induced vorticity (31) and the homogeneous solution,

$$\begin{aligned} \tilde{\omega}(x) &= \omega'_0 \int_0^x e^{-\frac{A}{\kappa}\xi^2} d\xi \\ &+ \chi'_0 \frac{\alpha g \sin \varphi}{A} \int_0^x d\zeta e^{-\frac{A}{2\kappa}\zeta^2} \int_0^\zeta d\mu \int_0^\mu d\xi e^{\frac{A}{2\kappa}\xi^2} \end{aligned} \quad (33)$$

Here the value for the parameter ω'_0 is chosen to cancel out the uniform vorticity of the solution (31). The form of this localized response vorticity matches the intuition that hot fluid goes up and cold fluid down. Such a localized vorticity structure associated with T-vorticity structure is one of the striking features of active scalar turbulence.

For any non-vanishing value of χ'_0 , $\chi_y(x)$ is an odd function having a double bump and consequently the temperature $\theta(x) = \theta(x=0) - \int_0^x \chi_y(\xi) d\xi$ forms a ridge. Such temperature ridges are often observed in DNS. However, far away from the origin, temperature diverges logarithmically. [12]. We think that the divergence at infinite distances is not necessarily pathological, since we are interested only in the local behavior of the structures (around the origin). Furthermore, this divergence prevents the strain of the external flow from squashing the temperature ridge. Like the FT type, the typical width of the vorticity structure is estimated as $\sqrt{\kappa/A}$. It is noted that this IT solution (30) is also the Burgers vortex layer solution to the three-dimensional barotropic vorticity equation. (Recall that the governing equation (5) for χ is the same as that of three-dimensional barotropic vorticity.)

III. EXTENSION

In this section, we consider the following external flow:

$$\Psi(x, y) = -A y f(x), \quad (34)$$

where $f(x)$ is a function satisfying a condition mentioned later. When $f(x) = x$, this flow becomes a stagnation flow. A major difference from the $f(x) = x$ cases is that the external flow (34) has in general non-zero vorticity,

$$\Omega(x, y) \equiv -\Delta \Psi = A y f''(x). \quad (35)$$

Thus Ω should satisfy the vorticity equation. We will discuss the realizability of (34) in detail later in this section.

Under the extended stagnation flow (34), we further assume functional forms of temperature and velocity as follows:

$$T(x, y, t) = \theta(x), \quad (36)$$

$$\begin{aligned} \mathbf{u}(x, y, t) &= (\partial_y \Psi, -\partial_x \Psi) + (0, v(x)) \\ &= (-A f(x), A y f'(x) + v(x)). \end{aligned} \quad (37)$$

Then χ and the total vorticity ω are given by

$$\chi(x) = (0, -\theta'(x)) \equiv (0, \chi_y(x)), \quad (38)$$

$$\omega(x, y) = -\Delta \Psi + v'(x) \equiv \Omega(x, y) + \tilde{\omega}(x). \quad (39)$$

We call $\tilde{\omega}$ response vorticity. The velocity field Eq. (37) is uniquely decomposed into the y -dependent and the y -independent parts.

Imposing the general boundary conditions

$$\chi_y(x=0) = \chi_0, \quad (40)$$

$$\chi'_y(x=0) = \chi'_0, \quad (41)$$

$$\tilde{\omega}(x=0) = \tilde{\omega}_0, \quad (42)$$

$$\tilde{\omega}'(x=0) = \tilde{\omega}'_0, \quad (43)$$

steady solutions to Eqs.(5) and (6) are easily obtained for any $f(x)$ as follows:

$$\begin{aligned} \chi_y(x) &= \chi_0 e^{-\frac{A}{\kappa} \int_0^x f(\lambda) d\lambda} \\ &+ \chi'_0 e^{-\frac{A}{\kappa} \int_0^x f(\lambda) d\lambda} \int_0^x e^{\frac{A}{\kappa} \int_0^\xi f(\lambda) d\lambda} d\xi, \end{aligned} \quad (44)$$

$$\begin{aligned} \tilde{\omega}(x) &= \tilde{\omega}_0 + \tilde{\omega}'_0 \int_0^x e^{-\frac{A}{\nu} \int_0^\zeta f(\lambda) d\lambda} d\zeta \\ &+ \frac{\alpha g \sin \varphi}{A} \int_0^x d\zeta e^{-\frac{A}{\nu} \int_0^\zeta f(\lambda) d\lambda} \int_0^\zeta \chi_y(\mu) e^{\frac{A}{\nu} \int_0^\mu f(\lambda) d\lambda} d\mu \\ &= \tilde{\omega}_0 + \tilde{\omega}'_0 \int_0^x e^{-\frac{A}{\nu} \int_0^\zeta f(\lambda) d\lambda} d\zeta \\ &+ \chi_0 \frac{\alpha g \sin \varphi}{A} \int_0^x \zeta e^{-\frac{A}{\nu} \int_0^\zeta f(\lambda) d\lambda} d\zeta \\ &+ \chi'_0 \frac{\alpha g \sin \varphi}{A} \int_0^x d\zeta e^{-\frac{A}{\nu} \int_0^\zeta f(\lambda) d\lambda} \\ &\times \int_0^\zeta d\mu \int_0^\mu d\xi e^{\frac{A}{\nu} \int_0^\mu f(\lambda) d\lambda} d\mu \end{aligned} \quad (45)$$

The last two terms of Eq.(45) represent the vorticity induced by the buoyancy.

Now we discuss the realizability of the external flow (34). If we claim that Eq. (35) is a steady solution of the barotropic two-dimensional vorticity equation

$$(\mathbf{U} \cdot \nabla) \Omega = \nu \Delta \Omega, \quad (46)$$

where $\mathbf{U} = (\partial_y \Psi, -\partial_x \Psi)$. Then the equation for $f(x)$ is

$$\frac{\nu}{A} f^{(4)}(x) + f(x) f^{(3)}(x) - f'(x) f''(x) = 0, \quad (47)$$

where $f^{(j)}(x)$ denotes the j -th order derivative. Equation (47) has been studied by many authors as a model of a flow near a rigid wall [13]. In Ref. [15] the authors, who were interested in the finite time blow-up of the solution, dealt with the time-dependent stream function $\Psi = -A y f(x, t)$ in a bounded domain and discussed asymptotic behavior ($t \rightarrow \infty$) of the solution to the equation for $f(x, t)$, the Proudman-Johnson equation [14]. They showed that every solution decays to zero as $t \rightarrow \infty$ with homogeneous boundary conditions.

Here instead of solving Eq. (47), we examine the realizability of the external field (34). We do not think that the flow (34) should be an exact solution of the vorticity equation (46). Rather, we assume that the flow (34) is formed by a larger scale flow in the turbulence field. That is, from a practical point of view, a steady solution subjected to an external flow is no more than a local model of coherent structures in the turbulent field, so that the external flow need not satisfy Eq.(46). Thus it may be possible to add an forcing term describing an effect of the larger scale motions to Eq.(46). Denoting the forcing term by $F(x, y)$, the equation for Ω (or $f(x)$) can be rewritten

$$(\mathbf{U} \cdot \nabla)\Omega = \nu\Delta\Omega + F. \quad (48)$$

Then the steady-state equation for the total vorticity (39) can be written

$$(\mathbf{u} \cdot \nabla)(\Omega + \vec{\omega}) = \chi_y(x)\alpha g \sin \varphi + \nu\Delta(\Omega + \vec{\omega}) + F, \quad (49)$$

which yields the equation for the response vorticity $\tilde{\omega}$

$$\frac{\nu}{A} \frac{d^2 \tilde{\omega}}{dx^2} + f(x) \frac{d\tilde{\omega}}{dx} = \chi_y(x) \frac{\alpha g \sin \varphi}{A}, \quad (50)$$

from which the solution (45) is obtained.

By substituting $f(x) = x$, it is easily checked that the solutions (44) and (45) contain Burgers vortex layer type solutions.

In the following, we show two examples of $f(x)$. Each has both FT and IT type solutions. As the first example, we deal with an external flow

$$f(x) = 4x^3 - 2x, \quad (51)$$

which itself has vorticity $\Omega(x, y) = 24Axy$. The stream lines of the external flow is shown in Fig. 5. Here we assume an additional forcing $F(x, y)$ that keeps the external field (51) steady. (Equation (48) prescribes the forcing as $F(x, y) = 192A^2x^3y$)

For FT type solutions, we impose the boundary conditions

$$\chi_y(x=0) = \chi_0 \neq 0, \quad (52)$$

$$\chi'_y(x=0) = \chi'_0 = 0, \quad (53)$$

$$\tilde{\omega}(x=0) = \tilde{\omega}_0 = 0, \quad (54)$$

$$\tilde{\omega}(x=0)' = \tilde{\omega}'_0 = 0. \quad (55)$$

The conditions for the vorticity Eqs.(54) and (55) are chosen again to reflect only the effect of the buoyancy. The solutions (44) and (45) are then reduced to

$$\chi_y(x) = \chi_0 e^{-\frac{\Delta}{\kappa}(x^4 - x^2)}, \quad (56)$$

$$\tilde{\omega}(x) = \chi_0 \frac{\alpha g \sin \varphi}{A} \int_0^x \xi e^{-\frac{\Delta}{\kappa}(\xi^4 - \xi^2)} d\xi. \quad (57)$$

These solutions are plotted in Fig. 6.

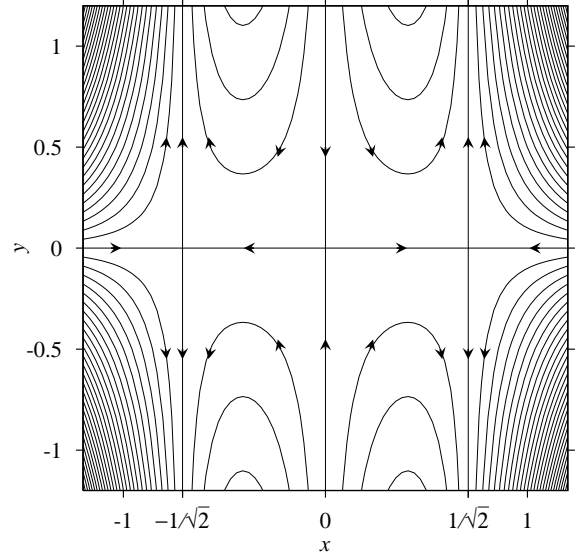


FIG. 5: Stream lines of an external flow $\Psi(x) = -y(4x^3 - 2x)$. The arrows denote the directions of the flow. Stagnation points are $(-1/\sqrt{2}, 0)$, $(0, 0)$ and $(1/\sqrt{2}, 0)$.

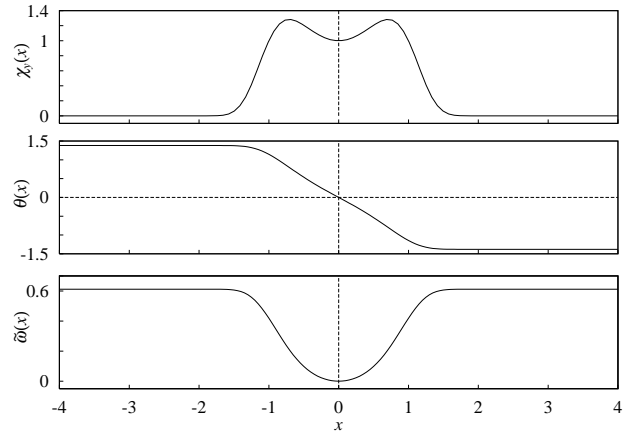


FIG. 6: FT type solutions for $\Psi(x) = -Ay(4x^3 - 2x)$: the T-vorticity (56), the corresponding temperature $\theta(x)$ and the response vorticity (57). Here we set the parameters as $A = 1$, $\kappa = 1$, $\alpha g = 1$, $\varphi = \pi/4$, $\chi_0 = 1$ and $\theta(x=0) = 0$.

For IT type solutions, we use the boundary conditions

$$\chi_y(x=0) = \chi_0 = 0, \quad (58)$$

$$\chi'_y(x=0) = \chi'_0 \neq 0, \quad (59)$$

$$\tilde{\omega}(x=0) = \tilde{\omega}_0 = 0, \quad (60)$$

$$\tilde{\omega}(x=0)' = \tilde{\omega}'_0 = 0. \quad (61)$$

Hence the solutions (44) and (45) is rewritten

$$\chi_y(x) = \chi'_0 e^{-\frac{\Delta}{\kappa}(x^4 - x^2)} \int_0^x e^{\frac{\Delta}{\kappa}(\xi^4 - \xi^2)} d\xi, \quad (62)$$

$$\tilde{\omega}(x) = \chi'_0 \frac{\alpha g \sin \varphi}{A} \int_0^x d\xi e^{-\frac{\Delta}{\kappa}(\xi^4 - \xi^2)}$$

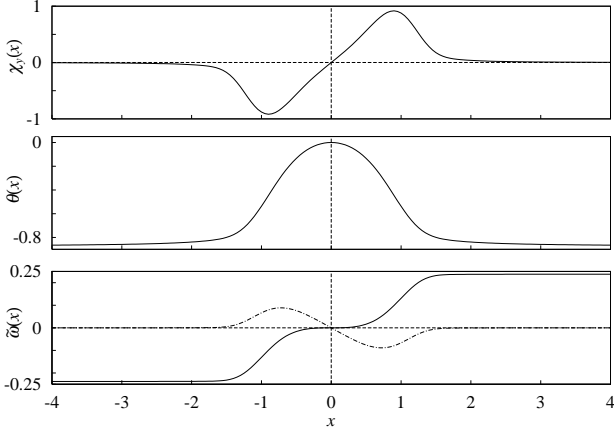


FIG. 7: IT type solutions for $\Psi(x) = -Ay(4x^3 - 2x)$: the T-vorticity Eq.(62), the corresponding temperature $\theta(x)$ and the response vorticity Eq.(63). Here we set the parameters as $A = 1, \kappa = 1, \alpha g = 1, \varphi = \pi/4, \chi'_0 = 1, \theta(x=0) = 0$, and $\tilde{\omega}'_0 = 0$. The temperature changes in a non-monotonic way. The dash-dotted line in the $\tilde{\omega}$ figure is a localized response vorticity obtained by setting $\tilde{\omega}'_0 = -0.172$.

$$\times \int_0^\zeta d\xi \int_0^\xi d\mu e^{\frac{A}{\kappa}(\mu^4 - \mu^2)}. \quad (63)$$

We plot the T-vorticity (62), the corresponding temperature $\theta(x)$ and the response vorticity (63) in Fig. 7. T-vorticity (62) has a double-bump for any non-vanishing χ'_0 . For this shape of the response vorticity (63), the vorticity-flux balance argument given in the previous section can be also applied. In addition, we can obtain a localized $\tilde{\omega}$ solution by adding the homogeneous solution of Eq.(50) in a similar way to the Burgers layer type solutions.

As an another example, let us consider the periodic flow:

$$f(x) = \sin x. \quad (64)$$

This flow has vorticity $\Omega = -Ay \sin x$. The corresponding forcing $F(x, y)$ is then $\nu Ay \sin x$. The streamlines of this external flow Eq.(64) are shown in Fig. 8, where stagnation points are located periodically.

For FT type solutions, we impose the boundary conditions (52)-(55). Then the general solutions (44) and (45) is expressed as

$$\chi_y(x) = \chi_0 e^{-\frac{A}{\kappa}(1-\cos x)}, \quad (65)$$

$$\tilde{\omega}(x) = \chi_0 \frac{\alpha g \sin \varphi}{A} \int_0^x \xi e^{-\frac{A}{\kappa}(1-\cos \xi)} d\xi. \quad (66)$$

They are plotted in Fig. 9. Multiple bumps in $\chi_y(x)$ are seen. From the monotonic behavior of the temperature which is similar to the Burgers T-vortex layer solution, these solutions (65) and (66) are classified to FT solutions. The remarkable feature of this solution is the

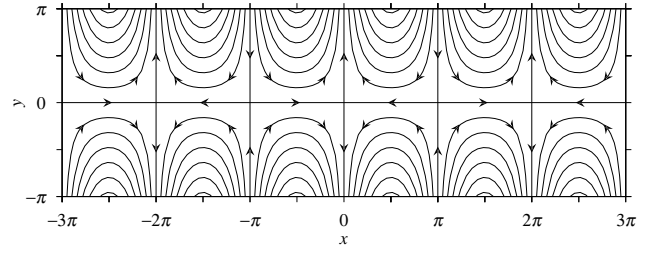


FIG. 8: Stream lines of an external flow $\Psi(x) = -y \sin x$. The arrows denote the directions of the flow. Stagnation points are $(n\pi, 0), n = 0, \pm 1, \pm 2, \dots$.

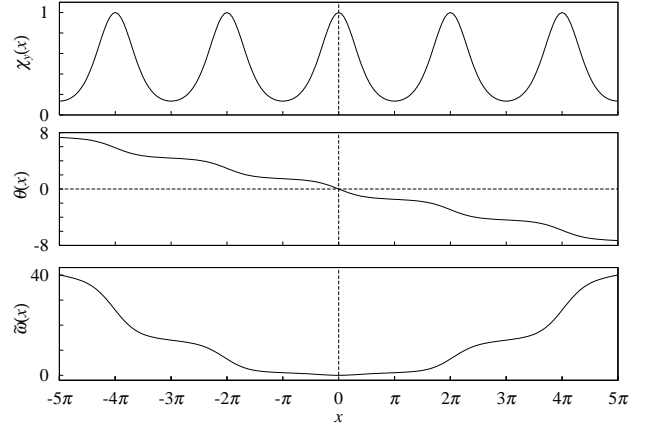


FIG. 9: FT type solution for $\Psi(x) = -Ay \sin x$: the T-vorticity Eq.(65), the corresponding temperature $\theta(x)$ and the response vorticity Eq.(66). Here we set the parameters as $A = 1, \kappa = 1, \alpha g = 1, \varphi = \pi/4, \chi_0 = 1, \theta(x=0) = 0$

staircase-like behavior of $\theta(x)$. This kind of staircase-like change of the temperature is sometimes observed in DNS. Hence the solution (65) and (66) can be useful to describe the small wavy behavior embedded on a temperature front.

To obtain IT type solutions, we use the boundary conditions (58)-(61). The solutions (44) and (45) are then expressed as

$$\chi_y(x) = \chi'_0 e^{-\frac{A}{\kappa}(1-\cos x)} \int_0^x e^{\frac{A}{\kappa}(1-\cos \xi)} d\xi, \quad (67)$$

$$\tilde{\omega}(x) = \chi'_0 \frac{\alpha g \sin \varphi}{A} \int_0^x d\xi e^{-\frac{A}{\kappa}(1-\cos \xi)} \times \int_0^\zeta d\mu \int_0^\xi d\xi e^{\frac{A}{\kappa}(1-\cos \xi)}. \quad (68)$$

These IT type solutions are shown in Fig. 10. Its temperature behavior is similar to the Burgers IT solution. The vorticity-flux balance argument can explain the shape of $\tilde{\omega}$ in this case as well. However the response vorticity (68) does not seem to converge as $x \rightarrow \pm\infty$, it would be no use considering the localized response vorticity in this case.

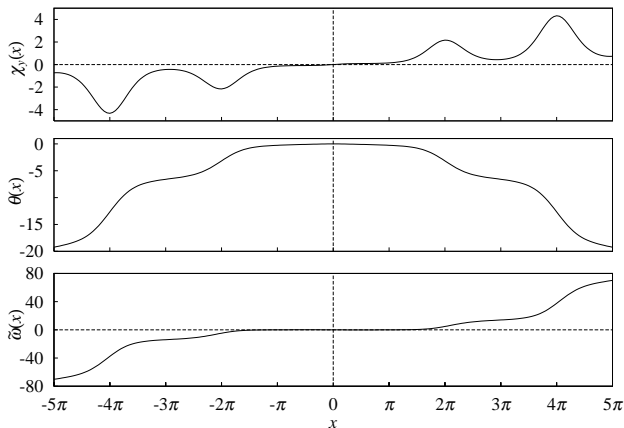


FIG. 10: IT type solutions for $\Psi(x) = -Ay \sin x$; the T-vorticity Eq.(67), the corresponding temperature $\theta(x)$ and the vorticity Eq.(68). Here we set the parameters as $A = 1, \kappa = 1, \alpha g = 1, \varphi = \pi/4, \chi'_0 = 0.1$ and $\theta(x = 0) = 0$.

IV. CONCLUDING REMARKS

We have examined a class of steady solutions to the two-dimensional Boussinesq approximation equations. We believe that these solutions well describe coherent structures observed in DNS of 2DFC. Under an extended stagnation flow $\Psi = -Ayf(x)$, we obtained two types of exact solutions; FT and IT types. In both cases, T-vortex layers are maintained steady by the balance between the strain of the external stagnation flow and the diffusion of T-vorticity. Furthermore, in the FT case a pair of T-vortex layers with opposite signs are annihilated by the compression of the extended stagnation flow without the continuous supply of T-vorticity which is maintained by the infinity of temperature at $x = \pm\infty$.

For the former (FT) type including the Burgers vortex layer type solution when $f(x) = x$, temperature remains finite as x goes to $\pm\infty$ and both T-vorticity and vorticity are localized around the origin. In contrast, for the latter (IT) type, the absolute value of temperature should diverge as x goes to $\pm\infty$ as mentioned above; T-vorticity

tends to zero quite slowly and vorticity is saturated to a finite value. If $f(x) = x$, T-vorticity takes at most two bumps. On the other hand, if $f(x) \neq x$ then it may take as many bumps as possible. although we only dealt with $f(x) = 4x^3 - 2x$ and $f(x) = \sin \varphi$ where two and infinite number of bumps are observed, respectively. These bumps seem to correspond to fine T-vortex structures observed in DNS of 2DFC turbulence.

So far we have taken for granted the independence of an external flow and a response. This view may be reasonable if we focus on local behavior of the coherent structures. Indeed the local shape of the structures are quite similar to the steady solutions. Thus it is suggested that the characteristic time scale of the external strain field are well separated from that of structure's motions. The role of the coherent structures on statistical properties of turbulence expected to be universal, is still an open question. Since the coherent structures have quite long correlation length comparable to the scale of the energy (temperature variance, i.e. entropy) containing range, their existence may break the locality hypothesis significantly. However, the authors have examined the relative diffusion in 2DFC turbulence recently and found that the coherent structures rather play an essential role in keeping the locality. These contradicting characteristics of the coherent structures make research on turbulence challenging.

In this sense, free convection turbulence is quite similar to 3DNS turbulence. We believe that coherent structures are universal and essential ingredients of turbulence. Therefore extensive researches on coherent structures are required.

Acknowledgments

This work has been partially supported by Grant-in-Aid for Science Research on Priority Areas (B) from the Ministry of Education, Culture, Sports, Science and Technology of Japan. Numerical computation in this work was carried out at the Yukawa Institute Computer Facility.

-
- [1] P. Cvitanović, *Universality in chaos*, (2nd edition Adam-Hilger, Bristol, 1989).
 - [2] E. D. Siggia, *Ann. Rev. Fluid Mech.* **26**, 137 (1994)
 - [3] A. Celani, A. Mazzino and M. Vergassola, *Phys. Fluids* **13**, 2133 (2001).
 - [4] D. Biskamp, K. Hallatschek and E. Schwarz, *Phys. Rev. E* **63**, 045302 (2001).
 - [5] V. S. L'vov, *Phys. Rev. Lett.* **67**, 687 (1991).
 - [6] S. Toh and E. Suzuki, *Phys. Rev. Lett.* **73**, 1501 (1994).
 - [7] S. Kida and M. Yamada, in *Turbulence and chaotic phenomena in fluids*, edited by T. Tatsumi (Elsevier Science Publishers B. V. (North-Holland), 1984), p. 275.
 - [8] P. Constantin, *SIAM Rev.* **36**, 73 (1994).
 - [9] T. S. Lundgren, *Phys. Fluids* **25**, 2193 (1982).
 - [10] M. Holzer and E. D. Siggia, *Phys. Fluids* **6**, 1820 (1994); [Erratum *ibid* **7** 1519 (1995)].
 - [11] S. Toh and T. Matsumoto, in *IUTAM Symposium on Geometry and Statistics of Turbulence* edited by T. Kambe et al. (Kluwer Academic Publishers, Dordrecht, 2001) p. 279.
 - [12] C. M. Bender and S. A. Orszag, *Advanced mathematical methods for scientists and engineers* (Mc-Graw Hill, New York, 1978) (reprinted by Springer-Verlag, New York, 1999), In Section 6.3, example 4 shows $\exp(-x^2) \int_0^x \exp(\xi^2) d\xi \approx 1/(2x)$ as $x \rightarrow \infty$.
 - [13] G. K. Batchelor, *An Introduction to fluid dynamics* (Cam-

- bridge University Press, Cambridge, 1967), Section 5.5, (b).
- [14] I. Proudman and K. Johnson, *J.Fluid Mech.* **12**, 161 (1961)
- [15] X. Chen and H. Okamoto, *Proc. Japan Acad.* **76**, 149 (2000)